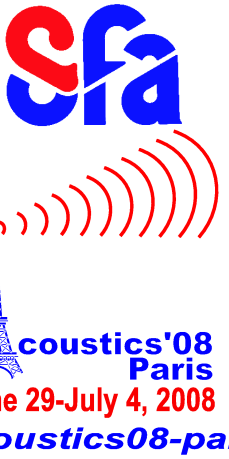

euronoise

Accoustic cleaning in nano-electronics

Paul Mertens

Imec, Kapeldreef 75, B-3001 Leuven, Belgium
paul.mertens@imec.be

State-of-the-art fabrication of electronic integrated circuits requires very high performance cleaning that is very selective with respect to the substrates and the fine features present on the surface. The use of high frequency acoustic excitation of the cleaning liquid could provide a possible solution to reach the specified cleaning targets. Current most advanced methods, however, do not provide the desired performance. This review covers different aspects. At first a description of the general issue in terms of trade-offs between particle removal capability versus the creation of damage is provided. The role of dissolved gas is covered. Also an appropriate formalism to describe the particle removal is explained. Finally a more detailed analysis of damage is presented.

1 Introduction

Fabrication of electronic integrated circuits, commonly referred to as micro-chips, has become a very large nano-electronics industry. The manufacturing process involves multiple cleaning steps (in the order of 100) in which very small contaminating residues such as particles or flakes with dimensions down to the order of ten or a few tens of nm need to be removed with very high efficiency Historically this was obtained by a pure chemical treatment in which particles were undercut by a weak etching (order of a few nm) of the substrate [1,2]. Thereby the Van der Waals attractive forces are reduced and electrostatic repulsive forces make the particle detach and transport away from the substrate. In state of the art and future nano-electronic devices the dimension of the structures are so small that the amount of substrate etching involved in a cleaning step should be kept below typically 0.05nm [3]. Therefore additional cleaning mechanisms involving a mechanical force have to be considered such as acoustic agitation of the cleaning liquid [4] or spraying liquid aerosol at high-velocity [5] onto the circuit surface. As these mechanical forces are engaged it was discovered that they also can damage fine structures already manufactured on the substrate, particularly if these are “up-features” sticking outward of the surface plane (Fig. 1) [6,7] (e.g. aggressively scaled shallow trench isolation features, gate stacks or BEOL dielectric lines).

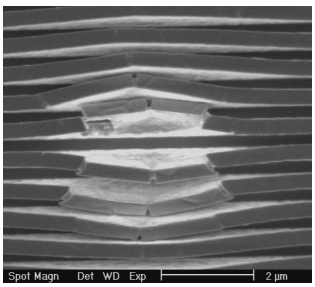

Fig. 1 Damage to Aluminum lines with a width of 0.25 um generated by megasonic cleaning [6].

This implies that a careful trade-off needs to be made between avoiding megasonic damage and still obtaining an acceptable cleaning performance. This challenge is schematically represented in Fig. 2 [8]. Suppressing the damage formation, and at the same time ensuring good and uniform particle removal requires the distribution of the forces induced by the cleaning events to be sufficiently narrow and well controlled. In state-of-the-art cleaning tools several factors contribute to the spread of the distribution of the cleaning events: spatial variations as well as power transients over time. Typically cleaning tanks used today tend to suffer from undesirable non-uniformity in the megasonic performance [9] while some alternative configurations feature improved uniformity (e.g. see below Fig. 10, for a single wafer system).

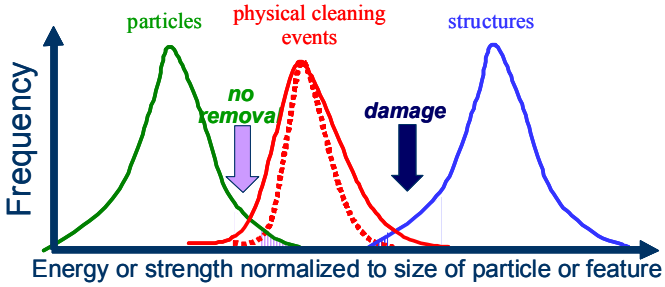

Fig. 2 Schematic diagram illustrating the process window for particle removal versus damage for physical assisted cleaning [8].

This review elaborates on the above mentioned trade-off. The effect of dissolved gas is discussed. A more formal treatment of particle removal is shown and finally a more detailed analysis of the damage is provided.

2 Trade-off

The trade off between the desired cleaning action and the undesired damaging of structures is shown in Fig. 3 for megasonic and liquid aerosol cleaning.

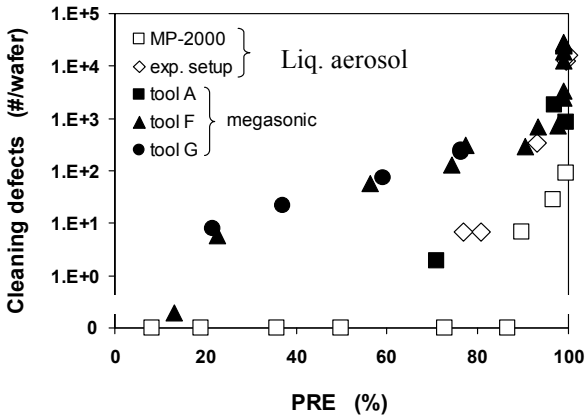

Fig. 3 Trade-off chart for number of cleaning defects to 70-nm poly-gate-stack lines vs. PRE for 78-nm silica particles on O3-last Si wafers. Results are shown for high-velocity liquid aerosol (nanospray) and megasonic cleaning. [10].

At first sight it may look that the liquid aerosol method performs better, than megasonic cleaning. One has to be very careful in generalizing these particular experimental findings. Several other consideration need to be taken into account. At first it should be realized that this first

comparative test was done with fairly large particles. Similar tests need to be repeated with more aggressively scaled features and particle sizes (< 50 nm). In addition, most of the megasonic systems show a considerable non-uniformity, which is believed to create inferior performance as some areas will be weakly cleaned and other areas with strong agitation may be heavily damaged already. It is believed that these are technical issues that could be overcome with good engineering, rather than being intrinsic fundamentals issues of megasonic agitation.

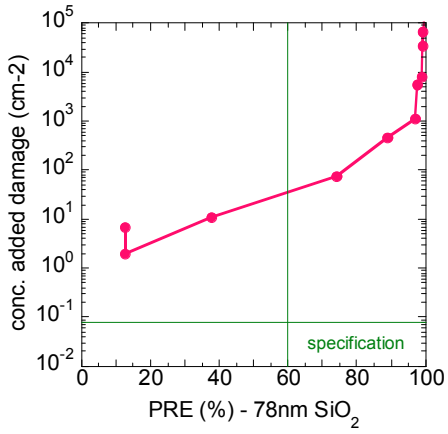

Fig. 4 Trade-off chart for surface concentraion of defects induced by cleaning to gate stack lines (width 25 nm, height: 50nm HM 100nm polySi 2.4nm SiON-deilectric) vs. removal efficiency for 78 nm silica particles (14hrs aged) for a state of the art cleaning technique. The right bottom rectangular area defines a specification used in development environment.

From Fig. 4 it is clear that with state-of-the art techniques the future cleaning targets cannot be accomplished. In order to be able to better fine tune and control megasonic cleaning much more basic understanding needs to be developed.

3 Cleaning mechanisms

A number of possible cleaning and damaging mechanisms have been proposed. Yet there is no clear general understanding of which mechanism is dominant under certain conditions. Here some observations are covered that could help to clarify the mechanisms.

Fig.5 shows that the amount of dissolved gas plays a major role for the particle removal [11, 12]. Particularly the removal efficiency of particles with a diameter below 200nm increases strongly with the concentration of dissolved gas. Therefore the removal of these particles has been attributed to the occurrence of cavitation.

Further investigations on the impact of gasification of the cleaning liquid on the performance of megasonic nozzle systems have been done [13]. Liquid solutions with a supersaturated gas content (X_c>1) were used by dissolving gas at high pressure. The pressure of the liquid is then reduced just before it enters the megasonic cleaning nozzle. It has been demonstrated that for a megasonic nozzle the removal efficiency for particles can be significantly enhanced by using this supersaturated condition. It was also found that this effect increases with increasing rotation speed of the wafer as shown in Fig. 6. It was found, however that damage to fine poly-silicon gate stack lines increases as well.

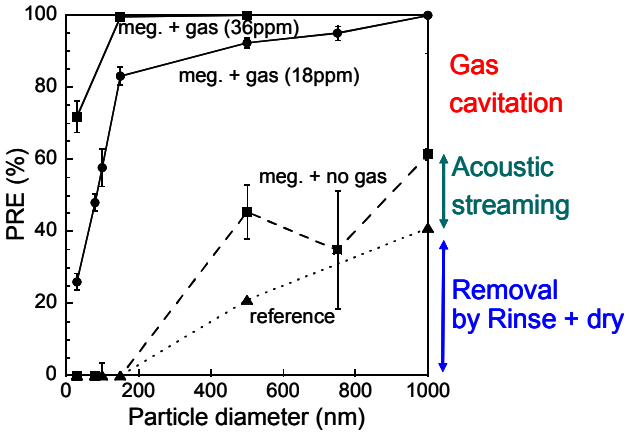

Fig. 5 Particle removal efficiency (PRE) as a function of particle diameter. SiO_2-particles are evaluated in 726 kHz wafer batch cleaning tank operating at its maximum power for different concentrations of dissolved gas in the liquid [12].

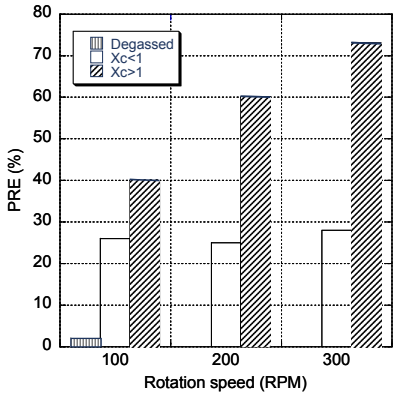

Fig. 6 Efficiency of removal of 78 nm SiO_2 particles obtained with a 1 MHz nozzle for 3 different normalized concentration levels of oxygen (X_c) present in UPW and for different wafer rotation speeds [13].

A lot of quantitative particle removal studies have been performed on blanket wafers. In reality wafers show topography. Therefore also particle removal from trenches was investigated for megasonic immersion tank cleaning and high-velocity liquid aerosol cleaning [14]. Relatively large trenches were used to allow for inspection of the particles from the trenches (depth 1 or 2.2 um, width: 10, 5, 2 and 1 um). It was found that a comparable reduction in particle removal performance is seen for megasonic cleaning (Fig. 7). For the liquid aerosol cleaning also the time dependence of the particle removal was studied by using different number of scans of the nozzle over the wafer [14]. This was modeled using the particle removal cleaning rate (explained below). It was found that the particles in the trenches are removed at a rate that is approximately 4 times lower than from flat blanket wafer surfaces, almost independently of the geometry of the trenches within the experimental parameter space.

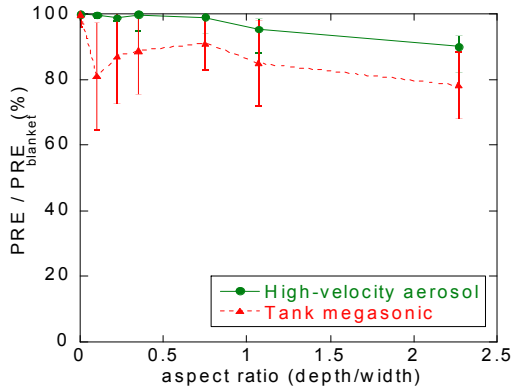

Fig. 7 Normalized particle removal efficiency for particles inside trenches as a function of the depth/width aspect ratio (zero corresponds to flat blanket wafers) [14].

4 Formalism for particle removal

The performance of cleaning processes is often quantified with (net) particle removal efficiency η. The definition of the net particle removal efficiency is:

$$\eta(t) = \frac{\sigma_0 - \sigma(t)}{\sigma_0} \qquad (1)$$

with σ_0 the initial surface concentration before cleaning and $\sigma(t)$ the instantaneous particle surface concentration at time t. As can be seen from eq. (1) the removal efficiency is a (usually increasing) function of the process time, t. This makes comparison of the intrinsic particle removal capability of different processes rather difficult unless the experimental results are obtained for the same process time. In order to improve cleaning performance for practical applications a better model description of the relation with the underlying microscopic phenomena needs to be made. Therefore a new metric was introduced that serves both purposes:

- being a good figure of merit for the process-time independent intrinsic particle removal performance of a cleaning process on one hand
- at the same time provide the ability to relate this intrinsic performance to the detailed microscopic cleaning phenomena on the other hand.

For that purpose the instantaneous *particle removal rate* (or removal frequency) has been defined as the particle removal flux normalized to the instantaneous particle surface concentration [15]:

$$f_{PR}(t) \equiv -\frac{1}{\sigma(t)}\frac{d\sigma(t)}{dt} \qquad (2)$$

If we assume that f_{PR} is constant over time this first order rate equation can be integrated to:

$$\eta_R = 1 - \exp(-f_{PR}t) \qquad (3)$$

The particle removal rate is the inverse of the average time that a particle remains bonded to the substrate surface , $t=1/f_{PR}$, while exposed to the cleaning process under study.

The relation to microscopic events that are responsible for cleaning action in a rather localized area is then given by:

$$f_{PR} = \Phi A \qquad (4)$$

Where A is the effective area on the wafer surface of the cleaning event and F is the flux of cleaning events on the surface

As mentioned above, a major issue in megasonic cleaning is the potential non-uniform cleaning performance. In order to get better understanding on the intrinsic behaviour more detailed studies need to be done that take into account the lateral variation, rather than work with average values for entire wafer surfaces. In that case the local particle removal rate f_{PR} is used.

As an example a cleaning process making use of a megasonic nozzle moving from center to edge with a constant speed, over a rotating wafer (1000 rpm) was characterized in more detail [16, 17]. The liquid was UP-water with a dissolved oxygen concentration at 20% of the saturation level in normal ambient conditions. Wafer maps of the local particle cleaning efficiency were made after different cleaning times, one of them shown in Fig.8. Making use of the rotational symmetry the radial position and cleaning time were transformed into a local dwell time of the nozzle resulting in the symbols on Fig. 9, which follow a common trend line. Expression (3) has been fitted to the experimental data of Fig. 9. This results in a good fit and yields a characteristic particle cleaning rate for this particular nozzle cleaning process of appox. 230 /s [16, 17]. The fitting proves the validity of this approach in which a set of experimental wafer maps is finally reduced to one single number.

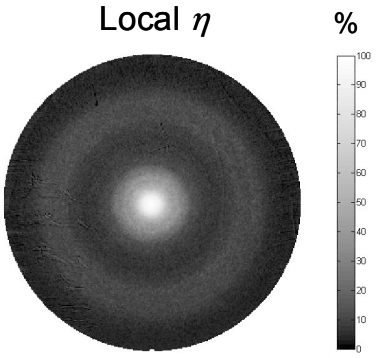

Fig.8: Wafer map (200mm diameter) of local particle removal efficiency $h(x,y)$ after 240s cleaning with a megasonic nozzle @1 MHz [17].

A similar analysis was applied to a single wafer system using a rod shaped megasonic device (Akrion Goldfinger) [17]. In this system the agitating rod extending from the center of the wafer to the edge, is held close above the wafer surface, while the wafer is rotating slowly. Water saturated with oxygen was applied. The particle removal efficiency was measured as a function of time in the range of 5 to 50 s. In such a system the local dwell time for the rod to the wafer surface decreases from the center toward the edge. The local particle removal rate (f_{PR}) was found to be highest at the edge and progressively decrease towards the center of the wafer as shown in Fig.10. The increase of f_{PR} with increasing radial distance compensates for the opposite radial dependence of the dwell time and results in an almost flat particle removal efficiency [17].

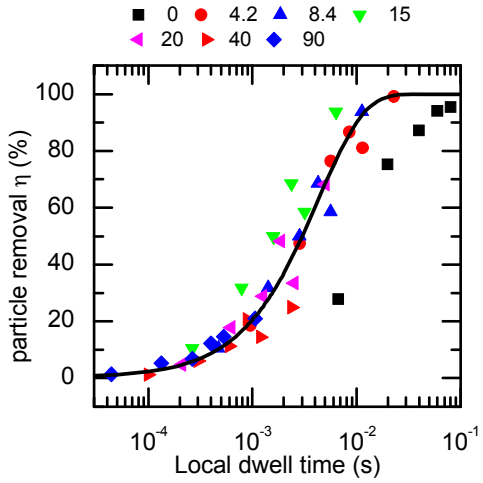

Fig. 9: Local particle removal efficiency for 78 nm SiO2 particles using a megasonic nozzle on a rotating wafer as a function of the local dwell time of the nozzle on one particular location of the wafer. Symbols represent experimental data. The solid line is the curve fit (eq. 3) yielding a particle removal rate of approximately 230/s [17]

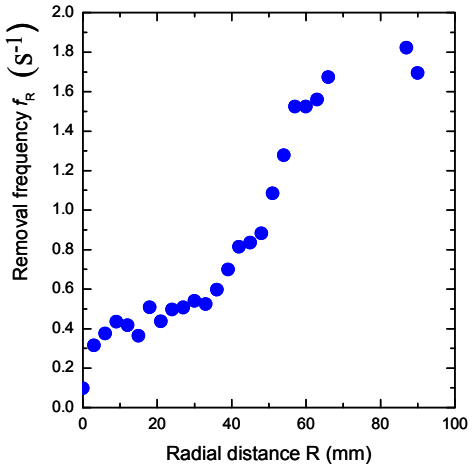

Fig. 10 Local removal rate (or frequency) obtained for a rod shaped megasonic device, as a function of radial distance. The increase with increasing radial distance compensates for the opposite radial dependence of the dwell time and results in a very good overall uniformity of cleaning [17].

5 Damage size and distribution

Based upon the shape of defects as shown in Fig.1 one can attribute the generation of defects due to the very strong (shear) forces induced by the jet, related to the asymmetric bubble collapse.

In order to try to better understand damage formation more detailed studies of lateral size and distribution of damage sites has been performed. The generation of defects by physical cleaning methods on patterned wafers was studied using test patterns with gate stack lines composed of an SiO2 hardmask on top of poly-crystalline silicon on top of SiON dielectric, with a total height of 150nm and a width of 20nm [18, 19]. Cleaning tests are performed on a prototype batch megasonic tool. Defect sites were detected using an automated optical bright-field inspection tool (KLA-Tencor 2351). Typically they consist of pieces of broken poly lines. For each defect the length of the part of the poly lines that was ripped out was measured using SEM. The histogram for the length of ripped off pieces is shown in Fig. 11. Typical lengths on the order of 0.5 to 1 mm were observed. For liquid aerosol cleaning the histogram was very similar with an additional weak tailing towards somewhat larger sizes.

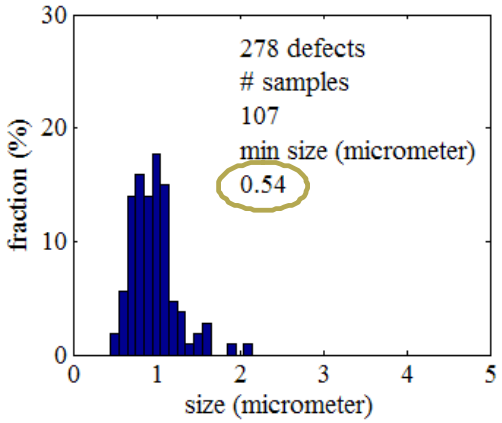

Fig.11: Distribution of length of damage parts of poly silicon test structure lines. for megasonic cleaning in an immersion tank [19].

The average defect density, $D_{\text{defect,aver}}$, is obtained by simply dividing the total number of defects in the inspected area by the inspected area. The value for $D_{\text{defect,aver}}$, is on the order of 6 /cm2.

On the wafer maps a large-scale (mm to cm range) non-uniformity is noticed. This non-uniform damaging is the clear fingerprint of a typical batch megasonic tool [9, 20, 21]. For the chip that has the highest defect density a defect density of 322 /cm^2 was obtained.

Furthermore also analysis was done on the lateral distribution. Detailed SEM review (FEI Expida 1285 or Hitachi S9380II) has been performed on randomly chosen defects (max 100).

It was noticed that defects tended to appear in clusters (on a mm scale). A quantitative analysis of the clustering tendency was performed. The defect clusters have a diameter of approximately 6 to 8 mm. The number of defects in a cluster was determined by considering defects separated less than 10µm to belong to the same cluster. Fig. 12 shows the distribution of the defect count per cluster for one condition of megasonic power, frequency and temperature. It can be seen that for different contditiona, all the damage clustering distributions tend to follow the same trend. Moreover, it can also be seen that a substantial portion (approx. 20%) of the inspected defects appears in a cluster with 2 or more defects.

If one would assume that within the defect cluster area, A_{clust}, defects would appear in random lateral position with a defect density $D_{\text{def,clust}}$ the likelihood to have k defects in a cluster can be described using a Poisson distribution as follows:

$$\frac{N_k}{N_{clust}} = e^{-A_{clust} D_{def,clust}} \cdot \left(\frac{\left(A_{clust} \cdot D_{def,clust}\right)^k}{k!} \right) \quad (5)$$

Where, N_k is the number of defect clusters with k defects and N_{clust} is the total number of defect clusters.

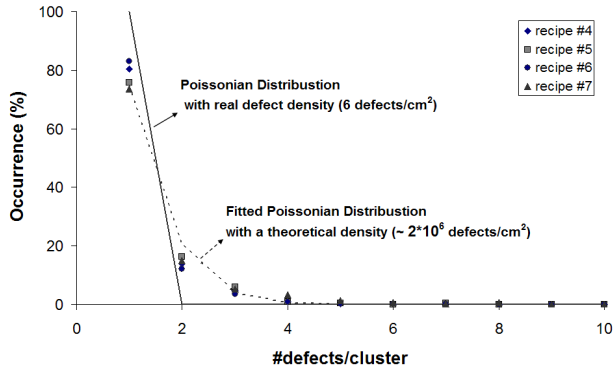

Fig. 12: Damage clustering distributions for different megasonic cleaning conditions. Poisson distribution fit the data only if a very high defect density (order 10^6 /cm^2) is used.

Fitting the experimental data yields a value for $D_{def,clust}$ on the order of 10^6 /cm^2 as shown in Fig. 12 This value is several orders of magnitude higher than the values obtained for the average defect density, $D_{defect,aver}$ mentioned above. This clearly proofs the existence of defect clusters on a micro-scale (about 10 mm).

Currently the mechanism behind the clustering is not clear. In this context it is interesting to note that clustering of defects in an annular pattern was also observed on planar aluminum substrates in case of single bubbles produced by laser at a controlled distance from the substrate [22].

In general, clustering could be attributed to a variety of mechanism that are related to

- the *nature of the cleaning events* (cavitation), that show some sort of clustering or interaction behaviour in time and/or in spcace: e.g. a break-up of the cavitation event into several subevents, the interaction between cavitation events (Bjerknes forces etc..), the formation of new bubbles after a collapse,…
- the *nature of the structures* that may show weak spots [19],
- *interactions between the cleaning events and the structures*:: e.g. the presence of a nucleation site on the structures, or the enchanced nucleation tendency on a broken structure, damage generated by a piece of material that is removed and impacts in a subsequent cleaning event.

5 Outlook

A lot more fundamental insight will be needed to fine-tune and control the strength of megasonic cleaning to the level it is required for future IC manufacturing. Also the use of megasonic agitation in non-aqueous liquid solutions needs to be studied as this has shown promising results for dedicated applications such as removal of photo-resist [23,24].

It is clear that a lot of experimental work has been performed along two different pathways: one more pragmatic macroscopic phenomenological approach, the other detailed microscopic studies of bubbles and related phenomena. By combining both efforts it should be possible to get better insight allowing to make major progress on the control of the processes. This should allow to design new megasonic systems that would satisfy the needs of future micro-electronic manufacturing standards.

References

[1] T. Hattori, Ed., *Ultraclean Surface Processing of Silicon Wafers*, Springer (1998).

[2] M. Meuris *et al., proc. ISSM*, p. 157 (1999).

[3] ITRS 2006 update: Front end process, table 68a&b, www.itrs.net.

[4] A. Mayer, and S. Schwartzman, *J. Electronic Materials*, 8: 855 (1979).

[5] I.Kanno, N.Yokoi, and K.Sato, *proc. ECS* **97-35**, p. 54.

[6] P.W. Mertens, *et al., Sol. State. Techn.,* 45:51 (2002).

[7] K.K. Christenson, *Proc. UCPSS2004*, Solid State Phenom. **103-104**, p.147 (2005).

[8] P. W. Mertens *et al.*, Proceedings of Technical Papers Internat. Symp. on VLSI Technology, Systems and Applications (VLSI-TSA), IEEE, 2006. pp.123-126; (24-26 April 2006; Hsinchu, Taiwan).

[9] G. Vereecke, *et al.*, *Proc. UCPSS 2004*, Solid State Phenom. **103-104,** p. 141, (2005).

[10] G. Vereecke, *et al.*, *Proc. UCPSS2006*, Solid State Phenom. **134**, p. 193 (2008).

[11] S. Cohen et al US patent 5,800,626 (1998).

[12] F. Holsteyns *et al., proc. ECS* **2003-26**, 161 (2003)

[13] F. Holsteyns *et al., Proc. UCPSS2006*, Solid State Phenom. Vol. 134, p. 201 (2008).

[14] K. Wostyn, *et al.*,. *ECS Transac.,* **11**(2), p. 55 (2007).

[15] T. Janssens *et al.*, *Proc. of UCPSS2006*, Solid State Phenom. **134**, p. 233 (2008).

[16] Mertens *et al.*, 4th International Surface Cleaning Workshop Northeastern University, Nov. 2006, Boston, USA, www.cmc.neu.edu.

[17] T. Janssens *et al.*, *ECS Transac.,* **11**(2), p. 353 (2007).

[18] K. Wostyn *et al.*, *Proc. Sematech Surface Preparation and Cleaning Conference 2007*.

[19] C. DeMarco *et al.*, *ECS Transac.,* **11** (2):87 (2007).

[20] G. Vereecke *et al.*, *Micro* **22** (1), p. 57 (2004).

[21] Y. Hagimoto, K. Asada, H. Iwamoto, *ISSM 2005 IEEE International Symposium on Semiconductor Manufacturing. Conference Proceedings*, 13-15 Sept. 2005, San Jose, CA, USA.

[22] A. Philipp and W. Lauterborn, *J. Fuid. Mech*. **361**, p. 96 – 97 (1998).

[23] M. Claes *et al.*, *Proc. UCPSS2006*, Solid State Phenom. **134,** p. 325 (2008).

[24] P. W. Mertens, G. Vereecke and R. Vos, *Semiconductor Fabtech*, **31**, 86 (2006).